

Determination of the optical potential for elastic proton scattering on ${}^6\text{Li}$, ${}^{12}\text{C}$, and ${}^{14}\text{N}$ at 144 MeV

G. L. Moake*

Purdue University, West Lafayette, Indiana 47907

P. T. Debevec

Department of Physics, University of Illinois, Urbana-Champaign, Illinois 61801

(Received 16 July 1979)

Elastic scattering cross sections have been measured for ${}^{14}\text{N}$ with 144 MeV protons at laboratory angles between 5° and 58° . Optical model parameters for ${}^{14}\text{N}$ were determined from these data, and parameters for ${}^6\text{Li}$ and ${}^{12}\text{C}$ were determined from previously existing data at 144 MeV.

[NUCLEAR REACTIONS ${}^{14}\text{N}(p,p){}^{14}\text{N}$, $E_p = 144$ MeV; measured $\sigma(\theta)$; optical model] analysis for ${}^{14}\text{N}$ and existing ${}^6\text{Li}$ and ${}^{12}\text{C}$ data.]

I. INTRODUCTION

Optical model potentials determined from elastic scattering are often a necessary input for the calculation of inelastic scattering and transfer reactions. For light nuclei, interpolation of the potential parameters from those obtained from global fits by some empirically determined mass number and energy dependence has an uncertain accuracy. We required the optical potentials for proton elastic scattering on ${}^6\text{Li}$, ${}^{12}\text{C}$, and ${}^{14}\text{N}$ at 144 MeV for theoretical calculations of the (p,n) cross section.¹ Although accurate data for ${}^6\text{Li}$ and ${}^{12}\text{C}$ were available,² the ${}^{14}\text{N}$ cross section needed to be measured. All three elastic cross sections were analyzed with a relativistic optical model code using Woods-Saxon form factors. These potentials should be of use in the calculation of other inelastic transitions.

II. EXPERIMENTAL PROCEDURE

The experiment was done at the Indiana University Cyclotron Facility (IUCF) with the quadrupole-dipole-dipole-multipole (QDDM) magnetic spectrometer.³ The experimental procedures were similar to those used in a larger program of elastic scattering measurements.⁴ An array of three detectors was placed in the spectrometer focal plane, the first of which was a position-sensitive helical wire ionization chamber which was used for momentum analysis. Following this were a 6.3 and a 12.7 mm plastic scintillator, which provided ΔE signals used for particle identification. Real events in the array were determined by a fast coincidence between the detectors.

For angles greater than 10° , a 27 mg/cm² BN

target, milled from a larger piece, was used. At angles less than 10° , the boron and nitrogen peaks overlapped too much to permit a reliable determination of elastic yields. A 2.1 mg/cm² melamine target ($\text{N}_6\text{C}_3\text{B}_6$), evaporated onto a thin carbon foil, and a natural carbon target, pressed to 9.9 mg/cm², were used at these angles. The relative amount of carbon in the two targets was determined by data taken at 20° , where all of the elastic peaks were clearly separated. The number of nitrogen events was then found by subtracting the carbon yield from that of the melamine. Only very small beam currents were needed, and no degradation of the melamine target was observed.

The overall deadtime in the detectors and computer was determined by sending pulser signals through the electronics. The pulser was triggered by a monitor detector, whose count rate was approximately proportional to the instantaneous beam current. The number of pulser signals sent to the detector was scaled and compared to the number of pulser events in the acquired spectra. Deadtimes were typically less than 2%, although they were as large as 12% for angles less than 10° .

Peak areas were usually obtained by summing the events in the peak channels and subtracting a linear background, which was determined by the number of events on either side of the peak. However, for the BN target at angles less than 16° , two overlapping peaks on a quadratic background were fitted to the data in order to separate the boron and nitrogen peaks. The shape of these peaks was chosen from that of an isolated nitrogen peak at a slightly larger angle. In the few cases that overlapping peaks were fitted to the data, the statistical errors were increased in an attempt to account for the additional error involved in the

peak stripping. A 2% error was then added in quadrature to all statistical errors to account for other random errors, such as variations in target thickness with beam wobble.

III. OPTICAL MODEL ANALYSIS

The optical model analysis was carried out with the code SNOOPY6.⁵ The potential was parametrized by the following form ($\hbar=c=1$).

$$U(r) = U_C(r) - \frac{V}{1+e^x} - \frac{iW_S}{1+e^{x'}} + \frac{1}{m_r^2} (V_{SO} + iW_{SO}) \frac{1}{r} \frac{d}{dr} \left(\frac{1}{1+e^{x''}} \right) \vec{L} \cdot \vec{\sigma},$$

$$U_C = \begin{cases} Z_1 Z_2 e^2 \frac{[3 - (r/R_C)^2]}{2R_C}, & r < R_C = r_c A^{1/3} \\ \frac{Z_1 Z_2 e^2}{r}, & r > R_C \end{cases}$$

$$x = (r - r_O A^{1/3}) / a_O,$$

$$x' = (r - r_W A^{1/3}) / a_W,$$

$$x'' = (r - r_{SO} A^{1/3}) / a_{SO}.$$

The wave equation used was the relativistic version of the Schrödinger equation introduced by Goldberger and Watson.⁶ The radial part for the l th partial wave can be cast into the conventional (nonrelativistic) form⁶

$$\left[\frac{d^2}{d\rho^2} + 1 - \frac{U(\rho)}{\sqrt{s} - m_1 - m_2} - \frac{l(l+1)}{\rho^2} \right] u(\rho) = 0,$$

but with a renormalized total potential $U \rightarrow \gamma U$, with γ being defined by the relation

$$\gamma = \frac{2(\sqrt{s} - m_2)}{\sqrt{s} - m_2 + m_1},$$

$$s = (E_1 + E_2)^2 - (p_1 + p_2)^2,$$

$$\rho = kr, \quad k = m_2 p_{1L} / \sqrt{s}.$$

The subscripts 1 and 2 represent the projectile and target, respectively, and L represents the lab frame. E and p are the total energy and 3-momentum. Thus, s is the center of mass energy (relativistic scalar), and γ is close to, but not equal to, the usual relativistic γ factor E_{1L}/m_1 .

The parameters of the optical model potential were adjusted to give the best fit to the data. All of the optical parameters were varied except for the Coulomb radius, which was set approximately equal to r_O . The Coulomb radius was not varied since variations in it can be compensated for by small changes in the other parameters, resulting in essentially the same fit.⁷ Different sets of from one to six parameters were simultaneously varied until a minimum was found. Starting pa-

TABLE I. Optical potentials for ${}^6\text{Li}$, ${}^{12}\text{C}$, and ${}^{14}\text{N}$ at 144 MeV.

	${}^6\text{Li}$	${}^{12}\text{C}$	${}^{14}\text{N}$
V	16.96	17.24	16.77
r_O	1.110	1.158	1.264
a_O	0.713	0.632	0.587
W_S	10.78	9.55	9.38
r_W	1.000	1.186	1.250
a_W	0.855	0.843	0.854
V_{SO}	-3.86	4.43	2.93
W_{SO}	-2.796	-2.838	-2.786
r_{SO}	0.870	0.904	0.914
a_{SO}	0.862	0.548	0.477
r_C	1.12	1.17	1.17
γ	1.061	1.066	1.067
χ^2/pt	0.25	3.3	2.1

rameters for ${}^{12}\text{C}$ were taken from the potential of Roland *et al.* at 150 MeV.⁸ The ${}^{12}\text{C}$ results were then used as starting parameters for ${}^6\text{Li}$ and ${}^{14}\text{N}$.

IV. RESULTS AND CONCLUSIONS

The resultant optical potential parameters are listed in Table I along with the factor γ . They can

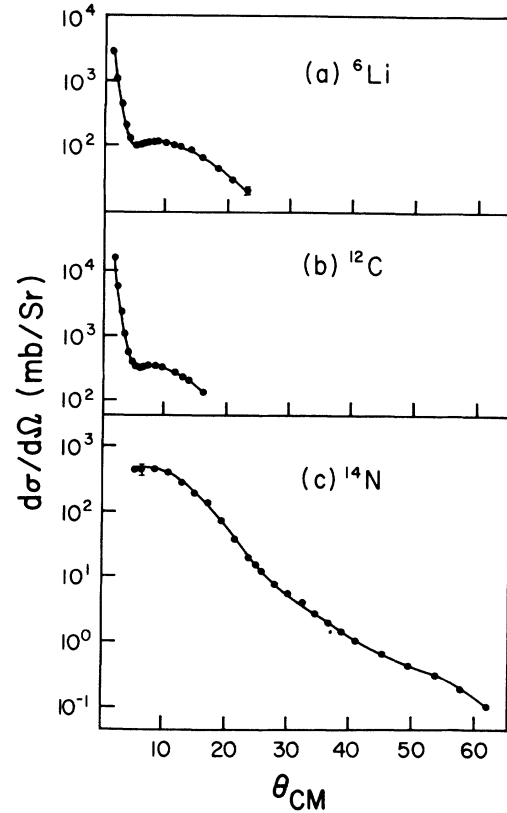


FIG. 1. Proton elastic scattering data for ${}^{14}\text{N}$ (this experiment), ${}^{12}\text{C}$ and ${}^6\text{Li}$ (Ref. 2). The line is an optical model fit using the parameters of Table I.

be used in a nonrelativistic code to a good approximation if realistic kinematics is employed and if all potentials are multiplied by the factor γ . Cross sections calculated from these potentials are shown in Fig. 1 along with the data.

The optical model calculations appear to reproduce the data well. For ^{12}C and ^{14}N the reduced χ^2 are similar to those obtained in the analysis of proton elastic scattering on heavier nuclei from a much larger data set.⁴ For ^6Li the reduced χ^2 is so small that it is quite probable that the parameters are poorly determined. In this regard, the negative value for the real part of the spin-orbit force must be interpreted as due to the small

angular range of the data. Calculations for which the spin-orbit potential is critical (for example, polarization studies) will be in error. No renormalization of the ^{14}N data would reduce the χ^2 of the final parameter set. The volume integrals of the real and imaginary central potentials are within the scatter suggested by studies on heavier nuclei⁴ for this bombarding energy, namely, $\gamma V_R/A \approx 200 \text{ MeV fm}^3$ and $\gamma V_I/A \approx 145 \text{ MeV fm}^3$, although the volume integral of the imaginary potentials is somewhat larger. These potentials are then a reasonable input for calculations requiring distorted waves.

*Present address: Indiana University Cyclotron Facility, Bloomington, Indiana 47405.

¹G. L. Moake, L. Gutay, R. P. Scharenberg, P. T. Debevec, and P. A. Quin, *Phys. Rev. Lett.* **43**, 910 (1979).

²O. N. Jarvis, C. Whitehead, and M. Shah, *Nucl. Phys.* **A184**, 615 (1972); AERE Report No. R6769, 1971.

³R. D. Bent, IUCF Int. Report No. 1-73 (unpublished); IUCF Techn. and Scient. report, (1976), p. 22.

⁴A. Nadasen, P. Schwandt, P. P. Singh, A. D. Bacher, P. T. Debevec, W. W. Jacobs, M. D. Kaitchuk, and J. T. Meek, *Phys. Rev. C* (to be published).

⁵P. Schwandt, IUCF Int. Report No. 77-8 (unpublished).

⁶M. L. Goldberger and K. M. Watson, *Collision Theory* (Wiley, New York, 1964).

⁷A. Nadasen, IUCF Int. Report No. 77-5 (unpublished).

⁸C. Rolland, B. Geoffrion, N. Marty, M. Morlet, B. Tatischeff, and A. Willis, *Nucl. Phys.* **80**, 625 (1966).